RSC Advances

PAPER

View Article Online
View Journal | View Issue

Cite this: *RSC Adv.*, 2018, **8**, 26934

(B,N)-Doped 3D porous graphene–CNTs synthesized by chemical vapor deposition as a bi-functional catalyst for ORR and HER†

Pingping Gao,[ab] Min Sun,[a] Xiaobo Wu,[*ab] Shuzhu Zhou,[b] Xiaoting Deng,[a] Zhiyong Xie,[*a] Li Xiao,[b] Lihui Jiang[c] and Qizhong Huang[a]

Received 12th May 2018
Accepted 10th July 2018

DOI: 10.1039/c8ra04048f

rsc.li/rsc-advances

Novel (B,N)-doped three-dimensional (3D) porous graphene–carbon nanotubes (CNTs) can be used as an excellent alkaline and acid tolerant electrocatalyst for both the oxygen reduction reaction (ORR) and the hydrogen evolution reaction (HER). Based on density functional theory, the H and O atoms' pre-and post-adsorption energy can effectively reduce the reaction energy barrier.

Introduction

Recently, graphene, with a one-atom-thick 2D honeycomb lattice of sp^2-bonded carbon atoms, has caught significant attention, because of its unique bonding structure, extremely high carrier mobility, bond-tuning capability, thermal transport properties, high chemical stability, *etc.* Therefore, graphene plays a dominant role in energy conversion and storage devices, such as fuel cells,[1] metal–air batteries[2] and oxygen sensors.[3] Chemically reduced graphene (rGO) is severely impaired due to abundant defects and chemical moieties created in the synthesis process, and it can easily agglomerate and stack by π–π interaction in the reduction process, resulting in slow transmittance and a decline in specific surface area.[5]

However, 3D graphene–CNTs exhibit strong direction-dependent thermal and electrical transport properties.[6,7] Theoretically, 3D covalently bonded graphene and CNT electrodes would extend these performances, which are propitious to energy storage and electrochemical sensing applications.[4,8] Moreover, graphene–CNT hybrid materials have several advantageous properties when used as electrodes, such as the large current density carrying capability and fast electron-transfer kinetics for nanoelectronic technologies.[8,9] In addition, CNT-based hybrid materials offer reduced reaction potentials, and minimum surface-fouling effects.[10] It should be noted that CNTs covalently bonded with graphene architecture can result in strongly direction-dependent thermal properties and extremely direction-dependent electrical transport properties.[11] Moreover, molecular dynamics simulation results showed that the covalently bonded graphene–CNT hybrid improved thermal transportation, and had a large surface area due to the stand-alone properties of the two materials.[11,12]

Heteroatom-doped carbon materials have been considered as one of the most suitable potential catalysts for ORR or HER in fuel cells because of their high catalytic activity and selectivity, strong durability, and low cost.[12–14] Their excellent electrocatalytic activity is mainly ascribed to the synergistic effect between carbon atoms and heteroatoms.[13,16] In view of this, N-VACNT,[17] (B,N)-VACNT[18] and (B,N)-graphene[19] have been studied, in which the electronic properties and chemical reactivity can be tailored. These atom-doped materials not only show a higher positive onset potential and electrocatalytic activity, but also possess fuel tolerance in an alkaline/methanol environment, long-term stability and high selectivity compared to the commercial Pt/C catalyst.[20] Importantly, doped graphene combined with CNTs as the active component has a tendency to enhance the electrocatalytic activity for ORR.[6] All of these characteristics allow the heteroatom-doped 3D graphene–CNTs to be an ideal substrate for catalyst particles. As a result of a strong interface connection, the catalyzed CNT growth on 3D porous graphene made by a CVD method has higher stability and a larger effective specific surface for ORR and HER. Unfortunately, studies show that the relationship between the base energy barrier and the catalytic activity is still not well understood, and catalyst durability is a major challenge for fuel cells. In addition, 3D graphene is rarely studied for ORR and HER. Therefore, further exploration of this new kind of substrate is highly desired.

In this study, we designed a simple but very efficient two-step CVD method to prepare a (B,N)-doped 3D porous graphene–CNT hybrid material (B–N–G–CNT), and studied its catalytic performance for ORR and HER.

[a]*State Key Laboratory for Powder Metallurgy, Central South University, Changsha 410083, P. R. China. E-mail: wuxiaobo176@126.com; xzy507@csu.edu.cn; qzhuang@csu.edu.cn; Fax: +86-731-88877671; Tel: +86-731-88877671*

[b]*College of Metallurgy and Materials Engineering, Hunan University of Technology, Zhuzhou, Hunan 412000, PR China*

[c]*College of Chemistry and Chemical Engineering, Central South University, Changsha 410083, P. R.China*

† Electronic supplementary information (ESI) available. See DOI: 10.1039/c8ra04048f

Experiments

3D graphene was synthesized by the method of CVD.[1,15] Firstly, 3D porous graphene was grown on nickel foam by CVD under ordinary pressure, using Ar as the carrier gas and ethanol as the carbon source. Secondly, the nickel foam was removed with 3 M HCl, and the 3D porous graphene with a continuous network was obtained. The preparation of the 3D B–N–G–CNT hybrid material was as follows: firstly, the 3D graphene foam was immersed in a 0.01 M H_3BO_3 and 0.01 M $Ni(NO_3)_2 \cdot 6H_2O$ mixed solution, washed and dried. Secondly, the sample was heated under NH_3/C_3H_6 ($V_{NH_3}/V_{C_3H_6} = 3:1$) at 800 °C for 0.5 h. Finally, the sample was put into 3 M HCl to completely dissolve the nickel.

Results and discussion

Fig. 1 shows the morphology of the B–N–G–CNT composite produced by the two-step CVD method. For the B–N–G–CNT composite, the graphene skeleton is fully and uniformly covered by the network of CNTs (Fig. 1a–d). The high-magnification SEM/TEM images reveal that the CNTs are about 50 nm in diameter, as shown in Fig. 1e. The CNTs provide a large accessible surface area of 3D structures in the B–N–G–CNT composite. The specific surface area of the B–N–G–CNT composite is evaluated by nitrogen adsorption (Fig. S1 in the ESI†). The results show that the Brunauer–Emmett–Teller (BET) specific surface area of the B–N–G–CNT composite is 32.987 $m^2 g^{-1}$, larger than that of B–N–G (2.629 $m^2 g^{-1}$).

It is indicated that the growth of CNTs can increase the BET specific surface area in B–N–G–CNT. Remarkably, N and B elements have been uniformly introduced into the 3D graphene–CNTs (Fig. 2).

To evaluate the catalytic activity of 3D B–N–G and the 3D B–N–G–CNTs, cyclic voltammetry (CV) in the potential range from −0.5 to +1.2 V was carried out in 0.1 M KOH solution under O_2/

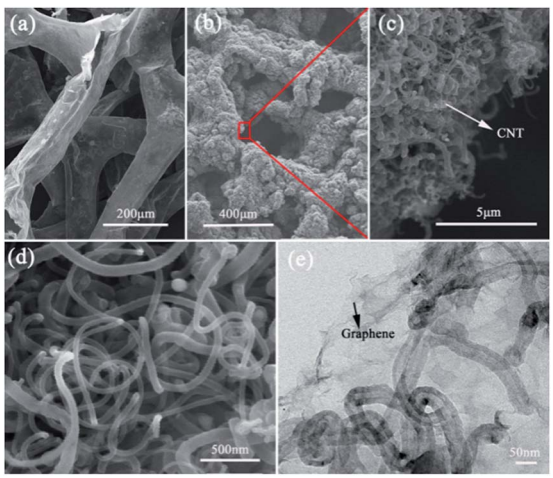

Fig. 1 Surface morphology of SEM images. (a) SEM images of B–N–G networks. (b) SEM image of B–N–G–CNT (c and d) SEM images of CNT. (e) TEM image of B–G–CNT.

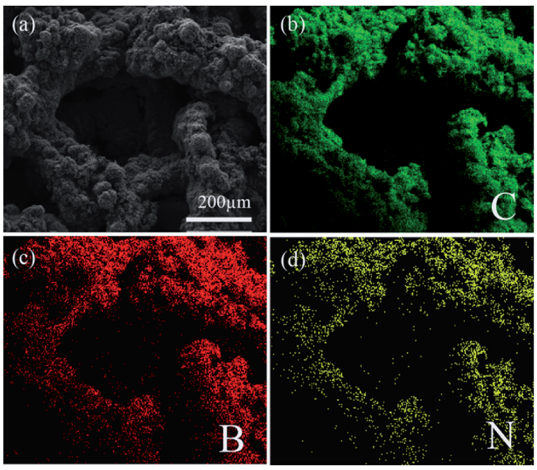

Fig. 2 SEM elemental mapping of (a) a typical SEM image, (b) C element, (c) B element, and (d) N element.

N_2-saturated conditions. It is noted that background correction of the capacitive currents was carried out for the RDE curves. It is clearly shown in Fig. 3a that the 3D B–N–G–CNTs have a higher onset potential and current densities than that of 3D B–N–G, which could likely be attributed to the synergistic effect of graphene and the CNTs. As shown in Fig. 3b, the half-wave potential and the onset potential of the B–N–CNTs is much more positive than that of B–N–G. Thus, the B–N–G–CNT electrocatalysts show a higher activity towards ORR in the present work.

Electrocatalytic HER activity of the B–N–G–CNTs and B–N–G on a glassy-carbon (GC) electrode was first investigated in acid solutions (0.1 M H_2SO_4) with a standard three-electrode system. The linear sweep voltammetry (LSV) polarization curves suggest that the CNTs grown on the B–N–G–CNT hybrid enhance the HER catalytic activity (Fig. 3c). Tafel plots for HER results reveal the electrode kinetics of these catalysts in the HER process. The linear portions of the Tafel plots (Fig. 3d) are fit to the Tafel equation yielding Tafel slopes of 119 mV dec^{-1} for the B–N–G–CNTs and 161 mV dec^{-1} (B–N–G). As per the Volmer mechanism, it is revealed that in this process, H_3O^+ ions are the proton source in acidic solutions (0.1 M H_2SO_4), and are rate-determining for the B–N–G–CNTs. In order to gain deeper insight into the excellent HER activity of the 3D B–N–G–CNTs, a durability experiment has been employed. The B–N–G–CNT composite exhibits superior durability in 0.1 M H_2SO_4 solution after 3500 cycles (Fig. 3f). In comparison with many literature results (Table S1 ESI†), the B–N–G–CNTs show excellent long-term cycling durability in the acid solution.

Theoretical method

In order to study the reference barrier of intermediate products, the HER reference barrier and the ORR reference barrier of three catalysts are examined by DFT, where X is the catalyst, representing the B–N–CNT, B–N–G and B–N–G–CNT catalysts in this work (Fig. S2 in the ESI†). These three kinds of catalyst can decrease the reference potential barrier of the HER and ORR at

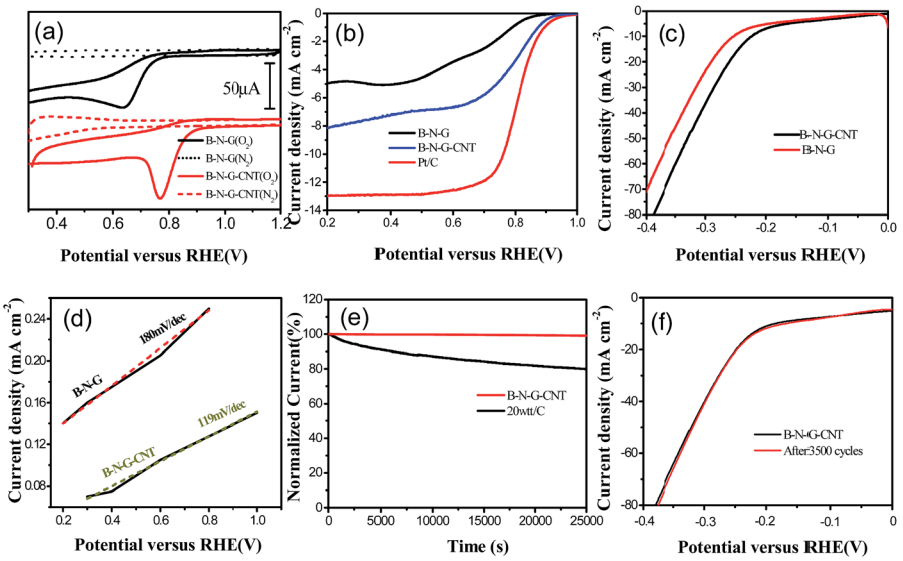

Fig. 3 Electrochemical tests (a) CV curves of 3D B–N–G and the 3D B–N–G–CNT hybrid in O_2/N_2-saturated 0.1 M KOH. (b) RDE curves of 3D B–N–G, 3D B–N–G–CNTs and Pt/C in O_2-saturated 0.1 M KOH. (c) HER performance of 3D B–N–G and the B–N–G–CNTs in 0.1 M H_2SO_4. (d) Corresponding Tafel plots for the HER in (c). (e) The durability of the B–N–G–CNTs in 0.1 M KOH. (f) The durability of the B–N–G–CNTs in 0.1 M H_2SO_4 solution.

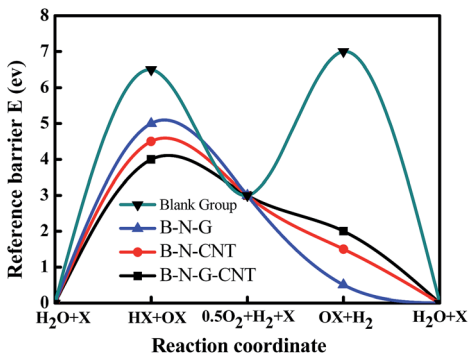

Fig. 4 Schematic diagram of the reaction path and reference barrier.

the same time, and the depressed barrier altitude of the reference potential barriers are 1.09948, 1.79397 and 2.40384 eV respectively. Because the B–N–G–CNTs barrier is the lowest among three catalysts, the B–N–G–CNT hybrid is the best catalyst for ORR and HER. The results agreed with our experiment very well. Based on the experimental data, it is inevitable that the intermediate products of N atoms and H atoms involved in the reaction can effectively reduce the reaction energy barrier (Fig. 4).

Conclusions

In conclusion, a novel (B,N)-doped three-dimensional (3D) porous graphene–CNT hybrid material has been fabricated by a chemical vapor deposition (CVD) and hydrothermal process. The (B,N)-doped 3D porous graphene–CNTs have an interconnected network, hierarchical pore structures and synergistic effect, a good doping ratio of (B,N) atoms, and excellent alkaline and acid tolerance for ORR and HER. The intermediate products of N atoms and H atoms involved in the reaction can effectively reduce the reaction energy barrier and enhance the catalytic activity. More importantly, the novel design can be applied to other catalytic materials.

Conflicts of interest

There are no conflicts to declare.

Acknowledgements

This work was supported by the National Key Research and Development Program of China (2016YFB0101310); the Natural Science Foundation of China (No. 21506258, 51774127) and the Natural Science Foundation of Hunan Province (No. 2016JJ3134) State Key Laboratory of Powder Metallurgy, Central South University. The calculations were completed in the High Performance Computing Center of CSU.

References

1 X. Li, W. Cai, J. An, S. Kim, J. Nah, D. Yang, R. Piner, A. Velamakanni, I. Jung and E. Tutuc, *Science*, 2009, **324**, 1312–1314.
2 H. Zhang, H. Li, H. Wang, K. He, S. Wang, Y. Tang and J. Chen, *J. Power Sources*, 2015, **280**, 640–648.
3 K. Gong, F. Du, Z. Xia, M. Durstock and L. Dai, *Science*, 2009, **323**, 760–764.
4 K. S. Novoselov, A. K. Geim, S. V. Morozov, D. Jiang, Y. Zhang, S. V. Dubonos, I. V. Grigorieva and A. A. Firsov, Electric Field Effect in Atomically Thin Carbon Films, *Science*, 2004, **306**, 666–669.

5 M. D. Stoller, S. Park, Y. Zhu, J. An and R. S. Ruoff, *Nano Lett.*, 2008, **8**, 3498–3502.
6 F. Du, D. Yu, L. Dai, S. Ganguli, V. Varshney and A. Roy, *Chem. Mater.*, 2011, **23**, 4810–4816.
7 V. Varshney, S. S. Patnaik, A. K. Roy, G. Froudakis and B. L. Farmer, *ACS Nano*, 2010, **4**, 1153–1161.
8 J. Kim, S. H. Bae, M. Kotal, T. Stalbaum, K. J. Kim and I. K. Oh, Soft but Powerful Artificial Muscles Based on 3D Graphene-CNT-Ni Heteronanostructures, *Small*, 2017, **13**, 31.
9 T. O. M. Samuels, A. W. Robertson, H. Kim, M. Pasta and J. H. Warner, *J. Mater. Chem. A*, 2017, **5**, 10457–10469.
10 Y. Shao, M. F. El-Kady, C. W. Lin, G. Zhu, K. L. Marsh, J. Y. Hwang, Q. Zhang, Y. Li, H. Wang and R. B. Kaner, *Adv. Mater.*, 2016, **28**(31), 6719–6726.
11 J. Chen, J. H. Walther and P. Koumoutsakos, *Adv. Funct. Mater.*, 2015, **25**, 7539–7545.
12 S. Liu, I. S. Amiinu, X. Liu, *et al.*, *Chem. Eng. J.*, 2018, **342**, 163–170.
13 Z. Kou, B. Guo, D. He, J. Zhang and S. Mu, *ACS Energy Lett.*, 2018, **3**(1), 184–190.
14 Y. Guo, P. Yuan, J. Zhang, *et al.*, *ACS Nano*, 2018, **12**(2), 1894–1901.
15 X. Wu, Z. Xie, M. Sun, T. Lei, Z. Zuo, X. Xie, Y. Liang and Q. Huang, *RSC Adv.*, 2016, **6**, 90384–90387.
16 S. Wang, L. Zhang, Z. Xia, A. Roy, D. W. Chang, J. B. Baek and L. Dai, *Angew. Chem., Int. Ed.*, 2012, **51**, 4209–4212.
17 B. J. Hinds, N. Chopra, T. Rantell, R. Andrews, V. Gavalas and L. G. Bachas, *Science*, 2004, **303**, 62–65.
18 S. Wang, E. Iyyamperumal, A. Roy, Y. Xue, D. Yu and L. Dai, *Angew. Chem., Int. Ed.*, 2011, **50**, 11756–11760.
19 Y. Xue, D. Yu, L. Dai, R. Wang, D. Li, A. Roy, F. Lu, H. Chen, Y. Liu and J. Qu, *Phys. Chem. Chem. Phys.*, 2013, **15**, 12220.
20 X. Wang, J. Wang, D. Wang, S. Dou, Z. Ma, J. Wu, L. Tao, A. Shen, C. Ouyang and Q. Liu, *Chem. Commun.*, 2014, **50**, 4839–4842.